Medium-range mid-tropospheric transport of ozone and precursors over Africa: two numerical case-studies in dry and wet seasons

B. Sauvage, F. Gheusi, V. Thouret, Jean-Pierre Cammas, J. Duron, J. Escobar, C. Mari, P. Mascart, V. Pont

Atmos. Chem. Phys. Discuss., 7, 4673–4703, 2007
www.atmos-chem-phys-discuss.net/7/4673/2007/

Atmospheric Chemistry and Physics Discussions

Medium-range mid-tropospheric transport of ozone and precursors over Africa: two numerical case-studies in dry and wet seasons

B. Sauvage, F. Gheusi, V. Thouret, J.-P. Cammas, J. Duron, J. Escobar, C. Mari, P. Mascart, and V. Pont

Laboratoire d'Aérologie, Toulouse, France

Received: 6 February 2007 – Accepted: 20 March 2007 – Published: 5 April 2007

Correspondence to: F. Gheusi (ghef@aero.obs-mip.fr)

Abstract

A meso-scale model was used to understand and describe the processes driving high ozone concentrations observed during both dry and monsoon seasons in monthly climatologies profiles over Lagos (Nigeria, 6.6° N, 3.3° E), obtained with the MOZAIC airborne measurements (ozone and carbon monoxide). This study focuses on ozone enhancements observed in the upper-part of the lower troposphere, around 3000 m. Two individual cases have been selected in the MOZAIC dataset as being representative of the climatological ozone enhancements, to be simulated and analyzed with on-line Lagrangian backtracking of airmasses.

This study points out the role of baroclinic low-level circulations present in the Inter Tropical Front (ITF) area. Two low-level thermal cells around a zonal axis and below 2000 m, in mirror symmetry to eachother with respect to equator, form near 20° E and around 5° N and 5° S during the (northern hemisphere) dry and wet seasons respectively. They are caused by surface gradients – the warm dry surface being located poleward of the ITF and the cooler wet surface equatorward of the ITF.

A convergence line exists between the poleward low-level branch of each thermal cell and the equatorward low-level branch of the Hadley cell. Our main conclusion is to point out this line as a preferred location for fire products – among them ozone precursors – to be uplifted and injected into the lower free troposphere.

The free tropospheric transport that occurs then depends on the hemisphere and season. In the NH dry season, the African Easterly Jet allows transport of ozone and precursors westward to Lagos. In the NH monsoon (wet) season, fire products are transported from the southern hemisphere to Lagos by the southeasterly trade that surmounts the monsoon layer. Additionally ozone precursors uplifted by wet convection in the Inter Tropical Convergence Zone can also mix to the ones uplifted by the baroclinic cell and be advected up to Lagos by the trade flow.

ACPD

7, 4673–4703, 2007

1 Introduction

Tropical ozone (hereafter O_3) controls atmospheric chemical composition and affects global climate and air quality through large scale redistribution. Over the Tropics, Africa is an important reservoir of ozone precursor sources allowing ozone to build up through active photochemistry exacerbated by high solar radiations. In particular, biomass burning products have substantial influence on O_3 mixing ratios Jonquières et al. (1998). These emissions account for half of the global carbon monoxide (CO) emissions (Andreae, Chapman and Hall, New York, 1993). Furthermore according to Marufu et al. (2000) pyrogenic emissions account for 16% of the ozone burden over Africa through different landtype burning (mostly savannas, forest and agricultural wastes) in the northern hemisphere from November to March and in the southern hemisphere from May to October. The dynamic processes allow redistribution of such emissions on a more global scale. During TRACE-A campaign, plumes loaded with high O_3 over the Atlantic were attributed to biomass burning emissions from Africa (Singh, 1996). More recently high CO mixing ratios over Indian Ocean have been attributed to African biomass burning (Edwards, 2006). It is then prominent to understand processes affecting redistribution of such emissions.

Over Africa like in other tropical regions a major circulation pattern is formed by the trade winds blowing from subtropical highs and converging towards the equator to form the Inter Tropical Convergence Zone (ITCZ) where vertical redistribution occurs. The continental north-easterly trade in north-hemispheric Africa is called Harmattan. Due to the shape of the continent a meridional land-sea constrast exists between western Africa and the Atlantic. This surface temperature gradient, that is especially enhanced during the northern-hemisphere summer (May to September), induces a south westerly monsoon flow affecting the Gulf of Guinea. During the same season the African Easterly Jet (AEJ), centred at 650 hPa, blows over north equatorial Africa (Hastenrath, 1985). The AEJ is maintained in association with two diabatically forced meridional circulations, one associated with deep convection (equatorward edge), the other to dry

ACPD
7, 4673–4703, 2007

convection (polerward edge), in the ITCZ and Saharan heat-low region respectively (Thorncroft and Blackburn, 1999; Parker et al., 2005).

According to Sauvage et al. (2005), biomass burning is responsible of high lower-tropospheric O_3 mixing ratios in monthly mean during dry (December to February, DJF) and monsoon (June to August, JJA) seasons, over West and Central equatorial Africa. The persistent O_3 enhancements were measured with the MOZAIC airborne programme downwind of emissions, and were related with a Lagrangian study to transport inside Harmattan and AEJ flows during dry season and inside trades flow during monsoon season. However it is not clear how air masses loaded with high O_3 and precursors can be measured near 600–650 hPa both in JJA and DJF, and particularly how they can be uplifted to the altitude of the AEJ during the dry season.

In the following study we investigate meso-scale processes controlling transport of surface biomass burning emissions in the upper part of the lower troposphere. We focus on two cases chosen in the MOZAIC database, as being representative of the O_3 enhancements during the dry and monsoon seasons, in terms of both dynamics and chemical structure of the atmosphere. For this purpose we adopt the approach of numerical modelling at the meso-α scale in association with on-line Lagrangian backtracking of airmasses (backtrajectories). The numerical set-up and Lagrangian method are described in Sect. 2. Sections 3 and 4 present the dry- and wet-season case-studies, respectively. The conclusions are summarized in Sect. 5.

2 Model specifications

The numerical simulations are performed with the MesoNH system – a non-hydrostatic anelastic mesoscale model jointly developed by the Laboratoire d'Aérologie (Toulouse, France) and CNRM (Météo-France). The dynamical core of the model is described in Lafore et al. (1998). A terrain-following vertical coordinate ($\hat{z}$) is used to include orography, based on altitude levels and the Gal-Chen and Sommerville (1975) transformation. Subgrid turbulence is parametrized with a 1-D, 1.5-order scheme using the turbulent

kinetic energy as prognostic value (Cuxart et al., 2000) and (Bougeault and Lacarrère, 1989) vertical-mixing length.

The warm-cloud microphysics scheme is of Kessler (1969) type including water vapour and liquid water in the form of non-precipitating cloud droplets or rain. Subgrid convection is parametrized with a 1D massflux scheme (Bechtold et al., 2001). The surface scheme is ISBA (Interactions between the Soils, Biosphere and Atmosphere), (Noilhan and Planton, 1989) and TEB (Town Energy Budget), (Masson, 2000). The radiation scheme is described in (Morcrette, 1991).

The trajectory calculations are based on an online method detailed in (Gheusi and Stein, 2002)(see also http://mesonh.aero.obs-mip.fr/mesonh/dir_doc/lag_m45_21mai2004/lagrangian_m45/). Complete references and comprehensive documentation can be found on http://mesonh.aero.obs-mip.fr.

In this study we use a model domain of 7500×7500 km^2 with a horizontal resolution of 50 km. The model has 72 stretched $\hat{z}$-levels up to 20 km, with a vertical resolution of 50 m near the surface gradually increasing to 400 m in the first 6 km. The time step is 90 s. ECMWF analyses are used for model initialization and lateral boundary coupling every 6 h.

3 Dry season case: 26–31 January 2002

3.1 In-situ MOZAIC profiles

The first studied case is motivated by the data of a MOZAIC aircraft landed at Lagos airport, Nigeria (6.6° N, 3.3° E), on 30 January 2002, around 17:00 UTC. Figure 1 shows the MOZAIC vertical profiles of chemical (O_3, CO and relative humidity) and dynamical parameters (wind direction and strength, potential temperature) recorded during the aircraft descent. Three polluted layers have been identified from these MOZAIC vertical profiles as described below.

A first layer (hereafter L1) below 850 m above sea level (a.s.l.) is a coastal boundary

layer with south-easterly (165°) wind of about 5 m/s and relative humidity around 50%. The CO mixing-ratio is maximum (1000–1400 ppbv). A steep gradient in ozone connects low values (30–40 ppbv) near the surface up to the high values (90 ppbv) on top. L1 is clearly vertically bounded from the capping airmass by a temperature inversion between 850 and 1000 m (visible in Fig. 1 as a sudden increase of θ and sudden drop in relative humidity and rotation of wind).

A stable layer (L2) is present between 1000 and 2000 m a.s.l., delimited below and above by temperature inversions. The dry (humidity less than 45%) north to north-easterly flux (10°–60°) is typical of the Harmattan flow. The O_3 and CO mixing-ratio are high (80–95 ppbv and 600–800 ppbv, respectively).

A relative minimum of O_3 separates L2 from the third layer of interest (L3) above, between 2100 and 4100 m a.s.l.. L3 is driven by a wind easterly jet (75–95°) – the AEJ – peaking at 15 m/s at about 2300 m a.s.l.. Ozone mixing-ratio ranges between 50 and 80 ppbv.

Within few kilometres above these three layers, O_3 and CO are more homogeneously distributed with typical "background" values (50 and 110 ppbv, respectively) measured at these altitudes in monthly average (Sauvage et al., 2005).

The characteristics of L1 and L2 are interpretable as follows. L1 is formed by a coastal airmass that has recently transited at low levels over the Gulf of Guinea. The high CO is likely due to offshore oil-fires as well as local emissions from the densely urbanized coastal area. The O_3 gradient can reflect surface deposition and destruction processes by concentrated nitrogen oxides (expected to accompany the CO emission). L2 shows the highest O_3 concentration but less CO (nevertheless exceeding 600 ppbv) than L1. This chemical signature reflects older airmass, driven by the Harmattan from inland where biomass burning has been detected by the satellite ATSR (http://dup.esrin.esa.int/ionia/wfa/index.asp) and MODIS (http://modis-fire.umd.edu/data.asp) instruments in the preceeding days.

Above these layers the origin of high O_3 in L3 (a climatological feature) is not as

straighforward to explain. In particular, how ozone and precursors are injected into the AEJ? Recent and local pollution can be excluded because of the low CO concentration – close to the tropospheric "background".

Note that the monthly climatological study of Sauvage et al. (2005) was only showing two O_3 layers: a surface layer (L1) with a steep gradient, and a thick maximum of O_3 corresponding to both the Harmattan and AEJ layers. L3 has however distinct source and origin, as it will be demonstrated now by means of a numerical model.

3.2 Model evaluation

The model started about 4 days before the MOZAIC flight landed, on 26 January 2002, 12:00 UTC, and ran during 102 h until 30 January, 18:00 UTC. Such a duration allows transport at the continental scale. In this section we check whether the model has not dynamically departed from ECMWF analyses and MOZAIC observations.

Figure 2 represents a comparison of the model vs. analysis wind field on 30 January 18:00 UTC (+102 h) at z=3000 m, corresponding to L3(AEJ). This dynamical structure appears to be correctly generated by the model. The maximum wind values are however higher in the model than in the analysis.

Figure 3 represents modelled vertical profiles of wind at Lagos, superimposed to the MOZAIC data. The simulated wind is smoother (broader extrema and of less amplitude) than the MOZAIC wind due to coarser vertical resolution in the model (50 to 400 m) than for the sampling of MOZAIC data (30 m). However the major features for wind speed (Fig. 3a) are well captured: low wind in layer L1, minimum just below 1000 m, wind around 7–8 m/s in L2, maximum (AEJ, layer L3) at about 2500 m (however with some underestimation). A second maximum centred at 3500 m is simulated higher (4500 m) by the model. The largest deviation from observed wind occurs between 7000 and 11 000 m but the dynamics at those levels is out of interest in this study. Moreover it must be kept in mind that a MOZAIC vertical profile corresponds for the aircraft to a horizontal path of few hundred kilometres, so the comparison makes little sense for the highest levels. Regarding wind direction (Fig. 3b), the agreement is

rather good for L1 and L3. The easterly component in the Harmattan layer (L2) appears however overestimated in the model.

The model appears at least valid to investigate the mid-term (few days) origin of the airmass sampled at the level of the AEJ. To this purpose a study based on back-trajectories is presented in the following subsection.

3.3 Airmass origin

A bunch of 90-hr backtrajectories (i.e. back in time to the simulation start) ending above Lagos on 30 January 18:00 UTC in the altitude range 2800–3400 m (ozone maximum in L3) is presented in Fig. 4. The airmass appears to remain coherent over the period. On 27 January the particles are located to the south-west of Sudan at lower levels (900–2500 m). All the particles are uplifted of at least 1000 m between 27 January 18:00 UTC and 29 January 00:00 UTC. Then in the next two days they are transported westward quasi-horizontally by the AEJ up to Lagos.

The uplift (circle in Fig. 4a) occurs over south-western Sudan and eastern Central African Republic (CAR), a region of savanna fires (see http://dup.esrin.esa.int/ionia/wfa/index.asp; http://modis-fire.umd.edu/data.asp). This uplift can explain the injection of low-level species into the AEJ.

Figure 5a provides details of the dynamics at 1500 m a.s.l. with the vertical displacement of air parcel integrated over the 6 h preceeding 28 January 6:00 UTC. This diagnostic actually shows more coherent and significant structures than instantaneous vertical velocity (highly variable spatially and temporaly). A sharp line of ascent meanders from southern Sudan to Nigeria through CAR and Cameroon. It is doubled on its southern side by a broader region of subsidence. The ascent line also marks the southern limit of the Harmattan (north to northeasterly wind). Finally it coincides with the the isoline θ_e 336 K (Fig. 5b), used by some authors (Jonquières et al., 1998) to delimit the Inter Tropical Front (ITF).

In this case the uplift is not induced by humid convection, rare during the dry season. Indeed the 3 h infra-red METEOSAT data (not shown) does not show clouds during that

period. The ITCZ extends to the south of the ITF, in the humid sector of the equatorial forest. Moreover no convective process occured in the model at the place and date of the particle uplift.

Figure 6 represents meridian vertical cross-sections of wind and potential temperature. It provides more details on the dynamics related to the ascent line and to the AEJ. The wind component in the vertical plane (vertical component of vectors exaggerated for visibility) clearly exhibits a closed vertical circulation on the southside of the ascent line, with the low-level branch (ground level–1000 m a.s.l.) oriented northwards and the return branch in altitude (1500–3000 m) southwards. The dipolar line ascent/subsidence depicted in Fig. 5a corresponds to the upward/downward branches. The potential temperatures (Fig. 6b) highlights the baroclinic nature of this circulation in response to surface gradient of temperature (the warm region being to the north) opposite to those of humidity and biomass cover.

The whole pattern should be viewed as a baroclinic solenoidal circulation (to some extent comparable to a coastal sea breeze but at a larger horizontal scale, of about 500 km). The AEJ is located just above the return branch and indeed corresponds to the geostrophic adjustment (thermal wind balance) to the northward horizontal gradient of temperature (visible below 2500 m a.s.l. in Fig. 6b) causing the circulation. The dynamics depicted here is in full agreement with the dynamical model proposed for the maintainance of the AEJ by (Thorncroft and Blackburn, 1999) by means of an idealized two-dimensional numerical model, and confirmed by (Parker et al., 2005) based on high-resolution dropsonde measurements.

Finally the ascent line is much thiner and stronger than the descending branch. This is due to the low-level convergence (below 1000 m a.s.l.) of the southerly "breeze" and northerly Harmattan flows.

In conclusion the path taken by the studied bunch of trajectories – namely uplift from the low levels in the ITF then transport by the AEJ – can explain the strong concentration of O_3 in the AEJ over equatorial West Africa highlighted by the MOZAIC climatology. In effect the described scenario does not rely on particular features of the

studied case, but on a quasi-stationary low-tropospheric circulation with a wide zonal extension over almost all the continent. Hence this scenario has a high potential of reproductibility.

4 Wet season case: 11–14 July 2003

In their monthly climatology for the JJA season, Sauvage et al. (2005) found two distinct wind regimes and accompanying ozone distributions (their Fig. 15). In this section we analyze a case study representative of the "polluted" regime, covering 28% of cases in JJA 2003 (the other 72% are less interesting because no polluted layer is present). One must however remark that in 2003 especially few ozone- and CO-rich layers were detected. Indeed recent weekly ozonesonde measurements from Cotonou (Benin) performed in 2005 and 2006 in the framework of AMMA (http://amma-international.org; contact:valerie.thouret@aero.obs-mip.fr) showed that polluted layers are encountered in 45% of cases.

4.1 MOZAIC profiles

Figure 7 displays O_3, CO, wind parameters, and potential temperature for the descent phase of the Frankfurt-Lagos flight landed on 14 July 2003, 15:30 UTC. No relative humidity data is available for this flight.

Below 2000 m the monsoon layer (L1) is characterized by oceanic southwesterly wind (around 225°). Inside L1 appears a 700 m-depth well-mixed layer (see θ and O_3). The 7 m/s jet near the surface is probably the signature of a local sea breeze that adds to the larger scale monsoon flux. This surface layer has no clear chemical signature, with a strong CO gradient (150–400 ppbv) but very low O_3 concentration (less than 20 ppbv). Offshore plaform fires can explain the CO maximum at low levels inside the monsoon flow. The low O_3 concentration excludes the possibility of a chemically mature airmass. So L1 probably shows clean oceanic air perturbed by local and recent

emissions.

The interesting layer in terms of medium-range transport of pollutants extends between 2000 and 4000 m a.s.l. (L2). The south-easterly 10–14 m/s flux corresponds to the northern extension of the southern-hemisphere trades surmounting the low-level monsoon layer (as shown in the following). L2 presents both high O_3 (more than 100 ppbv) and CO (up to 300 ppbv). Considering the mixing ratio of O_3 and CO, L2 cannot be explained by local pollution and is more representative of mature airmass loaded with pollutants few days ago (Chatfield and Delany, 1990). A model approach at regional scale is used to precise the history of this airmass.

4.2 Model evaluation

The model started about 3.5 days before the MOZAIC flight landed, on 11 July 2003, 00:00 UTC, and ran during 96 h until 15 July, 00:00 UTC. Figure 8 shows a comparison at z=3000 m on 14 July 2003, 12:00 UTC, between the ECMWF analysis and MesoNH (after 84 h). The circulations at regional scale, and in particular the trade wind flow over the Gulf of Guinea (boxed in Fig. 8 – the feature of interest regarding transport, see Sect. 4.3), are correctly reproduced – with however some overestimation in strength.

Figure 9 shows a comparison for wind speed and direction above Lagos between MOZAIC and MesoNH. In contrast there is a poor agreement between observed and simulated wind. The model fails to reproduce some meso-scale features of the monsoon system such as the monsoon layer below 2000 m (L1). This might be due to insufficient resolution (here 50 km) or a too long run (3.5 days), but anyway it illustrates the limitations of current models to capture the complex dynamics of the West African monsoon system (Sperber and Palmer, 1996) implying interaction of processes at different scales (Redelsperger et al., 2002), such as convection, evaporation or turbulence (Rowell et al., 1995). For instance idealized 2-dimensional approaches e.g., (Peyrillé et al., 2006) have pointed out the high sensibility of the monsoon dynamics to some key features such as humid static energy distribution in the boundary layer (Wang and Eltahir, 2000), easterly waves, or horizontal advection of energies

(Chou and Neelin, 2003). Concerning layer L2 (O_3 maximum between 2000–4000 m), the model underestimates wind speed but wind direction remains in the correct south-east quadrant (90–180°). Moreover the pathway and source location of backtrajectories presented below (in Sect. 4.3) are typical for such ozone enriched layers, according to the climatology by Sauvage et al. (2005) carried out with a Lagrangian model based on analized ECMWF wind-fields (see their Fig. 15). Therefore reasonable confidence can be put in the model for providing the source location of airmasses at regional scale despite failures at meso-scale around Lagos.

4.3 Airmass origin

Figure 10 shows trajectories ending in the L2 layer at Lagos on 14 July 2003, 18:00 UTC. Two distinct groups of trajectories are clearly visible, with source locations both in Democratic Republic of Congo (DRC hereafter). For Group 1 – trajectories ending in the lower part of L2 – ascent from the surface occurs above the border between DRC and Congo, on 11 July, 00:00 UTC. Trajectories of Group 2 – ending in the upper part of L2 – are uplifted further south-east in DRC. Fire occurences were detected by ATSR between the 8th and the 12th of July for both ascent regions. DRC is a major place of biomass burning during July (http://dup.esrin.esa.int/ionia/wfa/index.asp; http://modis-fire.umd.edu/data.asp), which can supply the two airmasses with fire products.

The processes explaining the uplift of the two air masses (trajectory groups 1 and 2) to the altitude of transport by the south-easterlies are under consideration now. Figure 11a confirms the source location of Group 1 (at the Congo/DRC border) as an area where ascent exceeds 900 m within 6 h, allowing the uplift of fire products to an altitude of 2500 m on 12 July, 12:00 UTC. In the time interval (06:00–12:00 UTC) Fig. 11b reveals an accumulation of 10 to 12 mm of convective precipitation over the same area. Thus the ascent of Group 1 is driven by wet convection in the ITCZ.

The strong uplift (of 500 to 700 m within 6 h) affecting particle Group 2 is clearly visible in Fig. 12a. Unlike Group 1 it cannot be linked to deep convection for none occurs

at this time and place. The process generating this ascent line is actually, in mirror symmetry, the same as the baroclinic dynamics depicted in Sect. 3. Indeed Fig. 12b shows that this line coincides with a sharp meridional gradient of equivalent potential temperature (θ_e). The low values of θ_e (<335 K) are found to the south and representative of the warm and dry continental south-easterlies. The high values (>336 K) on the north side are typical of the equatorial forest.

Figure 13 is a meridian vertical section across the ascent line and gives more details on its dynamics. The line corresponds to the convergence near the surface of the south-easterlies to the south with (weak) northerlies to the north. A closed vertical circulation is clearly visible between 3° S–5° N and below 1500 m on the northside of the line. This circulation is symmetric to the solenoidal circulation depicted in Sect. 3, with its low-level branch oriented souhwards and its upper return branch northwards. Figure 13(b) highlights the baroclinic nature of the circulation in response to the surface potential temperature and equivalent potential temperature gradients.

Again this pattern – that drives the processes of fire-product injection in altitude – can be viewed as a baroclinic solenoidal circulation upon which the large-scale south-easterlies impige. In this case however the cell is weaker than in northern hemisphere during the dry season, because of weaker θ_e gradients. An easterly jet is nevertheless simulated above the return branch, between 2000–2700 m, corresponding to the geostrophic adjustement (thermal wind balance) to the meridional surface gradient of temperature. This jet has actually been observed with radio-sondes data by Burpee (1975) and Janicot (1993).

5 Conclusions

A meso-α model (MESO-NH) was used to understand and describe the processes driving high ozone concentrations observed during both dry and monsoon seasons in monthly climatologies of vertical profiles over Lagos, obtained with the MOZAIC airborne measurements (Sauvage et al., 2005). This study focuses on ozone enhance-

ments observed in the upper-part of the lower troposphere, around 3000 m. To that purpose two individual cases have been selected in the MOZAIC dataset as being representative of the climatological ozone enhancements, to be simulated and analyzed with on-line Lagrangian backtracking of airmasses.

The evaluation of the simulated dynamical fields with in-situ MOZAIC measurements and with ECMWF analysis has shown a good agreement for the dry season case. For the wet season there is less agreement, confirming some difficulties of current modelling to fully reproduce complex dynamical meso-scale systems such as the monsoon onset. However the signature of regional transport processes is correctly reproduced by the model, allowing to describe the processes responsible for ozone and carbone monoxide enhancement at Lagos during the two seasons.

This study points out the role of baroclinic low-level circulations present in the Inter Tropical Front (ITF) area, to uplift ozone precursors emitted by the surface (in particular from biomass burning) to higher altitude. These circulations are sketched in Fig. 14.

Two low-level cells (below 2000 m), in mirror symmetry to eachother with respect to equator, form near 20° E and around 5° N and 5° S during the (northern hemisphere) dry and wet seasons respectively. Meridionally they extend over few hundreds kilometres. They are caused by surface gradients – the warm dry surface being located poleward of the ITF and the cooler wet surface equatorward of the ITF. Those gradients induce in each hemisphere a thermal circulation cell around a zonal axis, with its lower branch pointing toward the dry region, i.e. poleward. Thorncroft and Blackburn (1999) and Parker et al. (2005) invoked this mechanism (in the northern hemisphere) as the cause of the African Easterly Jet, that develops aloft in geostrophic response to meridional temperature gradient in the low levels (thermal wind balance). In the southern hemisphere an easterly jet also exists Burpee (1975); Janicot (1993), however of lesser intensity and zonal extension.

A convergence line (often termed InterTropical Front (ITF) or Discontinuity (ITD), Parker et al. (2005) and references therein) exists between the poleward low-level branch of the thermal cell and the equatorward low-level branch of the Hadley cell

(namely the harmattan in the northern hemisphere, and south-easterlies in the southern hemisphere). Our main conclusion is to point out this line as a preferred location for fire products to be uplifted and injected into the lower free troposphere.

The free tropospheric transport that occurs then depends on the hemisphere and season. In the NH dry season, the AEJ allows transport of ozone and precursors westward to Lagos. In the NH monsoon (wet) season, fire products are transported from the southern hemisphere to Lagos by the southeasterly trade that surmounts the monsoon layer. Additionally ozone precursors uplifted by wet convection in the ITCZ can also mix to the ones uplifted by the baroclinic cell and be advected up to Lagos by the trade flow.

The scenarios of Fig. 14 are proposed on the base of two case studies only. However these cases were chosen to be as representative as possible of the climatology established by Sauvage et al. (2005). The stationary nature of the surface gradients, the quasi-stationary character of the low-tropospheric circulation, and its zonal quasi-uniformity (at least in the northern hemisphere between 10° E–30° E), further support the idea that those scenarios are representative of a climatology of transport in Africa.

Acknowledgements. The authors acknowledge MOZAIC funding agencies, the European Commision, CNRS (France), Forschungszentrum Jülich (Germany), Météo-France, EADS (Airbus) and the airlines (Air France, Lufthansa, Austrian Airlines, and former Sabena who carry free of charge the MOZAIC equipment and perform the maintenance). The numerical resources were provided by IDRIS (CNRS).

References

Andreae, M. O.: The influence of tropical biomass burning on climate and the atmospheric environment, Biogeochemistry of Global Change: Radiatively Active Trace Gases, edited by: R. S. Oremland, 113–150, Chapman and Hall, New York, 1993. 4675

Bechtold, P., Kain, J., Bazile, E., Mascart, P., and Richard, E.: A mass flux convection scheme for regional and global models, Quart. J. Roy. Meteor. Soc., 127, 869–886, 2001. 4677

Bougeault, P. and Lacarrère, P.: Parameterization of orography-induced turbulence in a meso-beta scale model, Mon. Wea. Rev., 117, 1870–1888, 1989. 4677
Burpee, R.: Some features of synoptic-scale waves based on a composing analysis at gate data, Mon. Wea. Rev., 103, 921–925, 1975. 4685, 4686
Chatfield, R. and Delany, A.: Convection links biomass burning to increased tropical ozone: However, models will tend to overpredict O3, J. Geoph. Res., 95, 18 473–18 488, 1990. 4683
Chou, C. and Neelin, J.: Mechanisms limiting the northward extent of the northern summer monsoons over North America, Asia, and Africa, jc ???, 16, 406–424, 2003. 4684
Cuxart, J., Bougeault, P., and Redelsperger, J.-L.: A turbulence scheme allowing for mesoscale and large-eddy simulations, Quart. J. Roy. Meteor. Soc., 126, 1–30, 2000. 4677
Edwards, D. P. e. a.: Satellite-observed pollution from Southern Hemisphere biomass burning, J. Geophys. Res., 111, doi:10.1029/2005JD006 655, 2006. 4675
Gal-Chen, T. and Sommerville, R.: On the use of a coordinate transformation for the solution of the Navier-Stokes equations, J. Comput. Phys., 17, 209–228, 1975. 4676
Gheusi, F. and Stein, J.: Lagrangian description of air-flows using Eulerian passive tracers, Quart. J. Roy. Meteor. Soc., 128, 337–360, 2002. 4677
Hastenrath, S.: Climate and circulations of the tropics, D. Reidel, Dordrecht, 1985. 4675
Janicot, S.: Variability of dynamical fields over Africa (1970–1988); atlas for validation of general circulation models, Tech Note LMD, 187, 131pp, 1993. 4685, 4686
Jonquières, I., Marenco, A., Maalej, A., and Rohrer, F.: Study of ozone formation and transatlantic transport from biomass burning emissions over West Africa during the airborne Tropospheric Ozone campaigns TROPOZ I and TROPOZ II, J. Geoph. Res., 103, 19 059–19 074, 1998. 4675, 4680
Kessler, E.: On the distribution and continuity of water substance in atmospheric circulation, Meteor.Monogr., 46, 165–170, 1969. 4677
Lafore, J., Stein, J., Asencio, N., Bougeault, P., Ducrocq, V., Duron, J., Fischer, C., Héreil, P., Mascart, P., Redelsperger, J., Richard, E., and Vilà-Guerau de Arellano, J.: The Meso-NH atmospheric simulation system. Part I : Adiabatic formulation and control simulations, Ann. Geophys., 16, 90–109, 1998, http://www.ann-geophys.net/16/90/1998/. 4676
Marufu, L., Dentener, F., Lelieveld, J., Andreae, M., and Helas, G.: Photochemistry of the African troposphere: Influence of biomass-burning emissions, J. Geoph. Res., 105, 14 513–

14 530, 2000. 4675
Masson, V.: A physically-based scheme for the urban energy balance in atmospheric models, Boundary Layer Meteorology, 94, 357–397, 2000. 4677
Morcrette, J.-J.: Radiation and cloud radiative properties in the European Center for Medium range Weather Forcasts forecasting system, J. Geoph. Res., 96, 9121–9132, 1991. 4677
Noilhan, J. and Planton, S.: A simple parametrization of land surface precessus for meteorological models, Mon. Wea. Rev., 117, 536–549, 1989. 4677
Parker, D., Thorncroft, C., Burton, R., and Diongue-Niang, A.: Analysis of the African easterly jet, using aircraft observations from the JET2000 experiment, Quart. J. Roy. Meteor. Soc., 131, 1461–1482, 2005. 4676, 4681, 4686
Peyrillé, P., Lafore, J.-P., and Redelsperger, J.-L.: An idealized framework to study the West African monsoon, Part I: Validation and key controlling factors, J. Atmos. Sci., in press, 2006. 4683
Redelsperger, J.-L., Diongue, A., Diedhou, A., Ceron, J.-P., Diop, M., Gueremy, J.-F., and Lafore, J.-P.: Multi-scale description of a Sahelian synoptic weather system representative of the West African monsoon, Quart. J. Roy. Meteor. Soc., 128, 1229–1257, 2002. 4683
Rowell, D., Folland, C., Maskell, K., and Ward, M.: Variability of summer rainfall over tropical North Africa, Quart. J. Roy. Meteor. Soc., 121, 669–704, 1995. 4683
Sauvage, B., Thouret, V., Cammas, J., Gheusi, F., Athier, G., and Nec, P.: Tropospheric ozone over Equatorial Africa: regional aspects from the MOZAIC data, Atmos. Chem. Phys., 5, 311–335, 2005, http://www.atmos-chem-phys.net/5/311/2005/. 4676, 4678, 4682, 4684, 4685
Singh, H. B. e. a.: Impact of biomass burning emissions on the composition of the South Atlantic troposphere: Reactive nitrogen and ozone, J. Geoph. Res., 101, 24 203–24 220, 1996. 4675
Sperber, K. and Palmer, T.: Interannual tropical rainfall variability in general circulation model simulations associated with the Atmospheric Model Intercomparison Project, jc, 9, 2727–2750, 1996. 4683
Thorncroft, C. and Blackburn, M.: Maintenance of the African easterly jet, Quart. J. Roy. Meteor. Soc., 125, 763–786, 1999. 4676, 4681, 4686
Wang, G. and Eltahir, E.: Biosphere-atmosphere interactions over West Africa. II: Multiple climate equilibria, Quart. J. Roy. Meteor. Soc., 126, 1261–1280, 2000. 4683

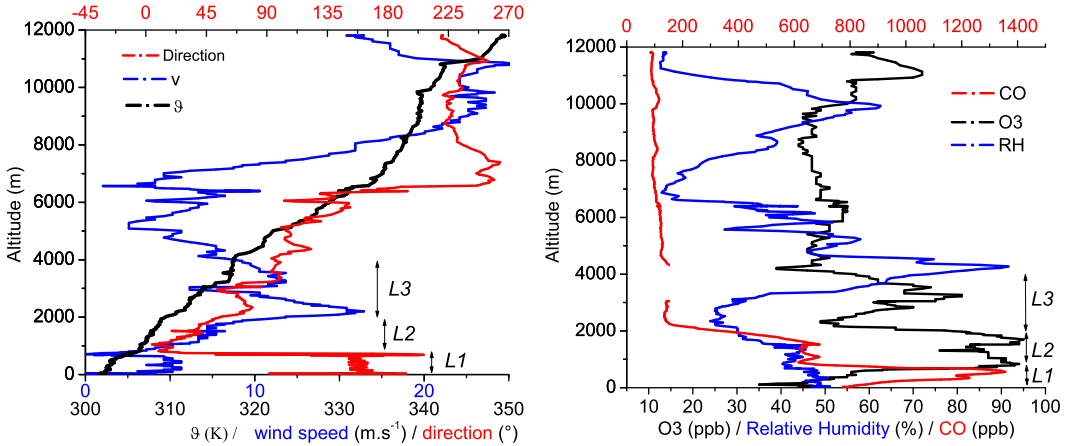

Fig. 1. MOZAIC descent profiles from the flight landed at Lagos airport on 30 January 2002, 17:00 UTC: potential temperature (θ), wind speed and direction (left panel); ozone (O_3) and carbon monoxide (CO) mixing-ratios and relative humidity (right panel).

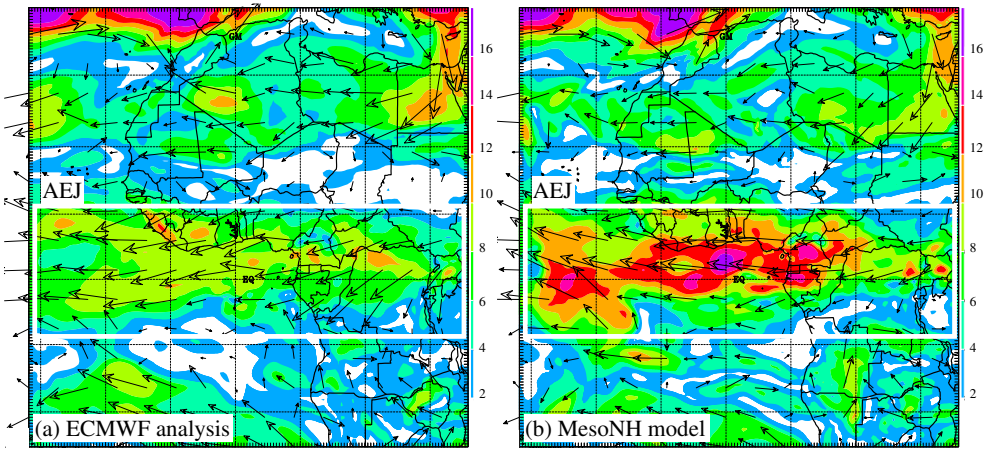

Fig. 2. Wind modulus (colorscale in m/s) and vectors at z=3000 m a.s.l. on 30 January 2002, 18:00 UTC: **(a)** ECWMF analysis; **(b)** MesoNH (+102 h).

ACPD
7, 4673–4703, 2007

EGU

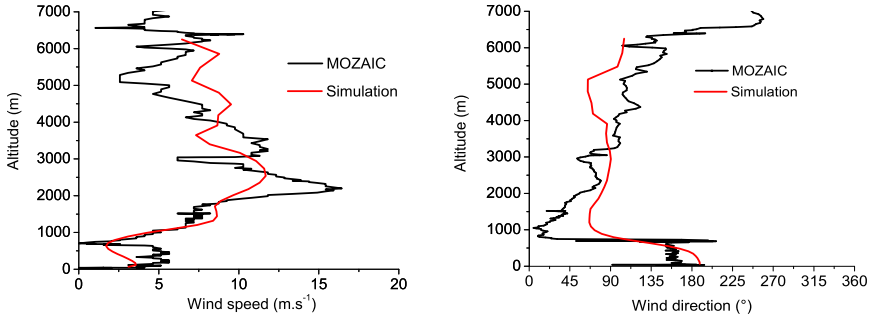

(a) (b)

Fig. 3. MOZAIC descent profile (black, landing 30 January 2002, 17:00 UTC) and simulated vertical profile over Lagos (red, 30 January 2002, 18:00 UTC): **(a)** wind speed (m/s); **(b)** wind direction (°).

ACPD
7, 4673–4703, 2007

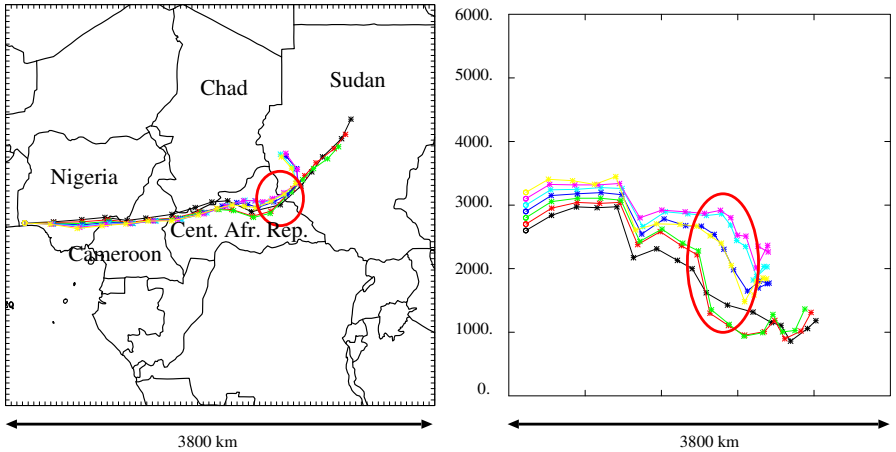

Fig. 4. Backtrajectories ending over Lagos on 30 January 2002, 18:00 UTC. Timestep: 6 h. Left panel: horizontal projection. Right panel: west-east vertical projection (altitude in m).

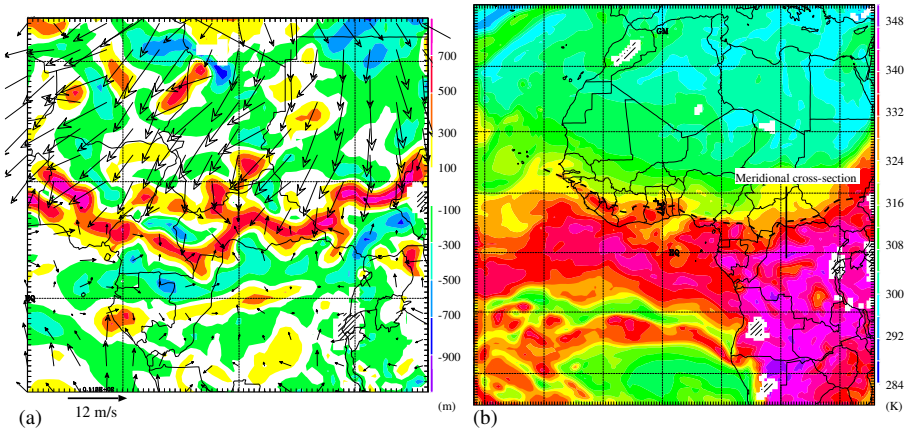

Fig. 5. **(a)** Air vertical displacement (m) on 27 January 2002 between 12:00 and 18:00 UTC at z=1500 m and wind vectors at 18:00 UTC 20 m above ground level. **(b)** Equivalent potential temperature (K) at 18 UTC, z=1500 m. The dashed line marks the intertropical front (ITF) and the solid segment locates the vertical cross-section considered in Fig. 6.

ACPD
7, 4673–4703, 2007

EGU

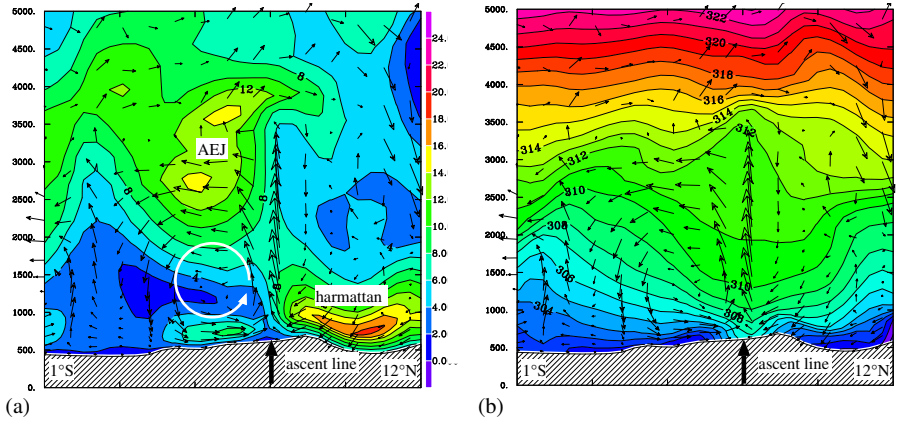

Fig. 6. Meridional vertical cross-section at 22° E (see location in Fig.5b) on 27 January 2002, 18:00 UTC. **(a)** Longitudinal wind component (vectors) and total-wind speed (colorscale in m/s). **(b)** Potential temperature (colorscale in K) – vectors as in (a).

ACPD
7, 4673–4703, 2007

EGU

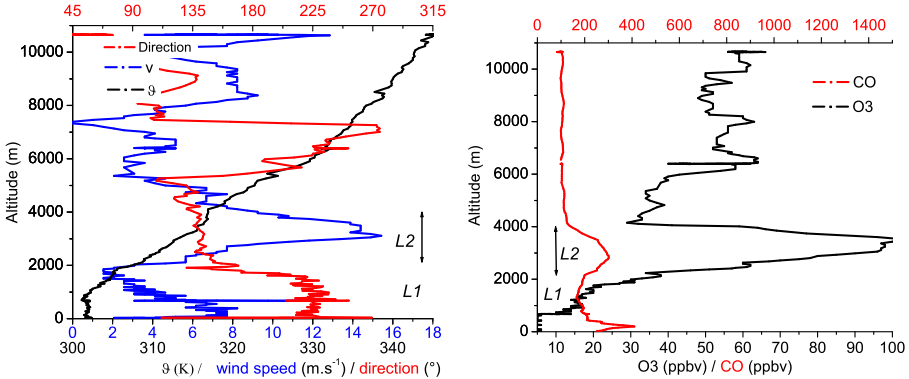

Fig. 7. MOZAIC descent profiles from the flight landed at Lagos airport on 14 July 2003, 15:30 UTC: potential temperature (θ), wind speed and direction (left panel); ozone (O_3) and carbon monoxide (CO) mixing-ratios (right panel).

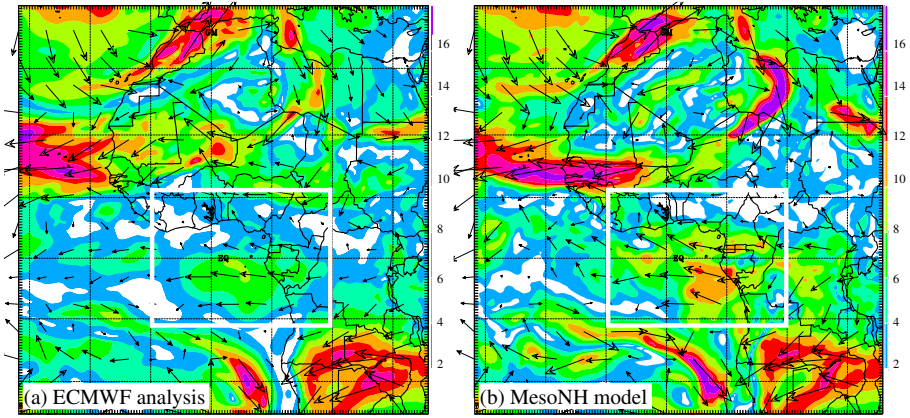

Fig. 8. Wind modulus (colorscale in m/s) and vectors at z=3000 m a.s.l. on 14 July 2003, 12:00 UTC: **(a)** ECWMF analysis; **(b)** MesoNH (+84 h).

ACPD
7, 4673–4703, 2007

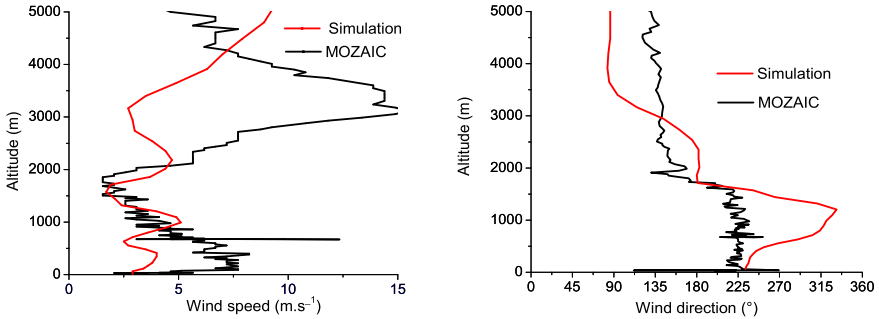

(a) (b)

Fig. 9. MOZAIC descent profile (black, landing 14 July 2003, 15:30 UTC) and simulated vertical profile over Lagos (red, 14 July 2003, 12:00 UTC): **(a)** wind speed (m/s); **(b)** wind direction (°).

ACPD
7, 4673–4703, 2007

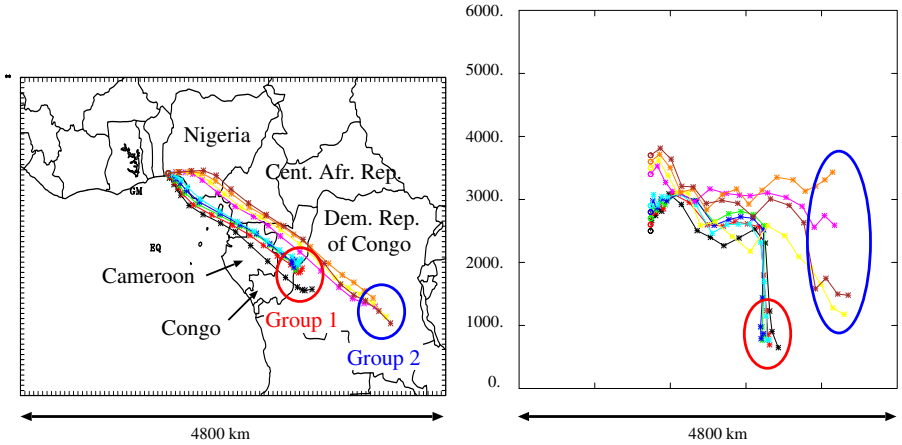

Fig. 10. Backtrajectories ending over Lagos on 14 July 2003, 18:00 UTC. Timestep: 6 h. Left panel: horizontal projection. Right panel: west-east vertical projection (altitude in m).

ACPD
7, 4673–4703, 2007

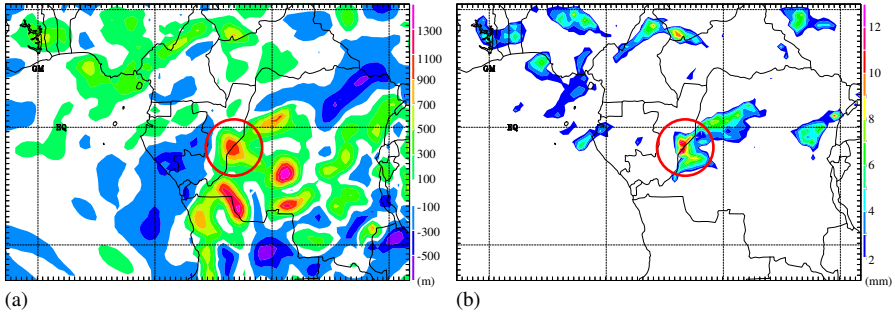

Fig. 11. **(a)** Air vertical displacement on 12 July 2003 00:00 UTC at z=2500 m, integrated over the 6 preceeding hours. **(b)** Convective precipitation on 12 July 2003 12:00 UTC accumulated over the 6 preceeding hours. The circle locates the ascent of particle Group 1 (see Fig. 10 and text).

ACPD
7, 4673–4703, 2007

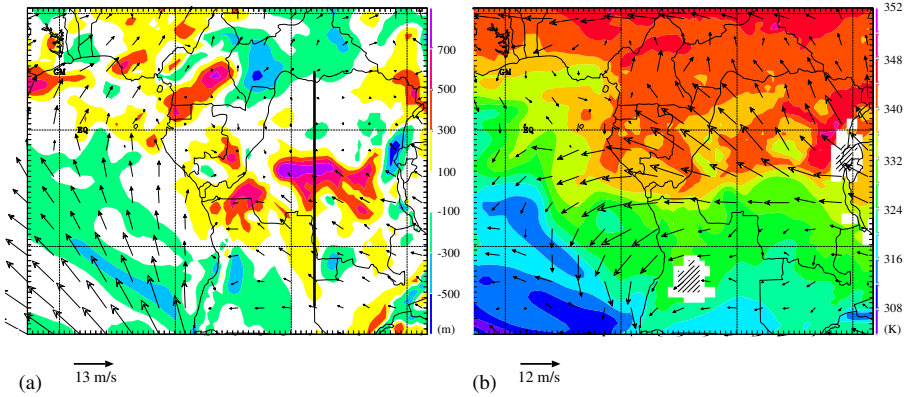

Fig. 12. **(a)** Air vertical displacement (m) on 11 July 2003 between 6 and 12:00 UTC at z=2000 m and wind vectors at 12:00 UTC 20 m above ground level. **(b)** 11 July 2003, 12:00 UTC: Equivalent potential temperature (K) at z=1500 m and wind vectors at z=2500 m. The solid segment locates the vertical cross-section considered in Fig. 13.

ACPD
7, 4673–4703, 2007

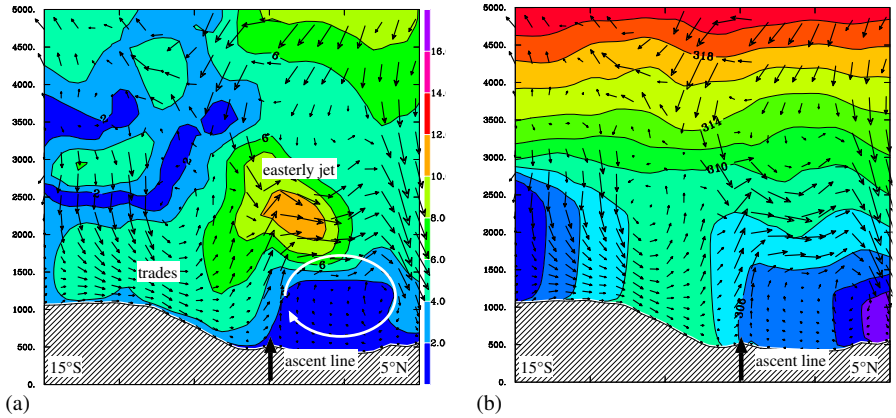

Fig. 13. Meridional vertical cross-section at 22E (see location in Fig.12a) on 11 January 2003, 12:00 UTC. **(a)** Longitudinal wind component (vectors) and total-wind speed (colorscale in m/s). **(b)** Potential temperature (colorscale in K) – vectors as in (a).

ACPD
7, 4673–4703, 2007

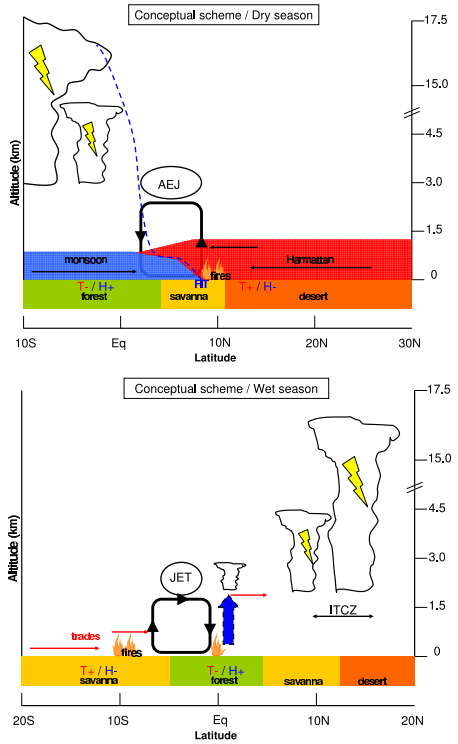

Fig. 14. Sketches for the injection of combustion products in the lower free-troposphere in Africa in the northern-hemisphere dry (DJF – fires in the NH – upper panel) and wet (JJA – fires in the SH – lower panel) season. The blue arrow (lower panel) symbolizes injection of pollutants by deep convection in the ITCZ.